European Journal of Pharmaceutics and Biopharmaceutics 197 (2024) 114233

Contents lists available at ScienceDirect

European Journal of Pharmaceutics and Biopharmaceutics

journal homepage: www.elsevier.com/locate/ejpb

Research paper

Azithromycin-loaded liposomes and niosomes for the treatment of skin infections: Influence of excipients and preparative methods on the functional properties

A. Abruzzo [a,*], R. Pucci [a], P.M. Abruzzo [b], S. Canaider [b], C. Parolin [a], B. Vitali [a], F. Valle [c], M. Brucale [c], T. Cerchiara [a], B. Luppi [a], F. Bigucci [a]

[a] Department of Pharmacy and Biotechnology, Via San Donato 19/2, University of Bologna, 40127 Bologna, Italy
[b] Department of Medical and Surgical Sciences (DIMEC), University of Bologna, Via Massarenti 9, 40138 Bologna, Italy
[c] Consiglio Nazionale delle Ricerche (CNR), Istituto per lo Studio dei Materiali Nanostrutturati (ISMN), via Gobetti 101, 40129 Bologna, Italy

ARTICLE INFO

Keywords:
Liposomes
Niosomes
Thin film hydration
Ethanol injection
Azithromycin
Retention studies
Antimicrobial activity
Cytotoxicity

ABSTRACT

The aim of this study was to develop azithromycin (AZT)-loaded liposomes (LP) and niosomes (NS) useful for the treatment of bacterial skin infections and acne. LP based on phosphatidylcholine from egg yolk (EPC) or from soybean lecithin (SPC), and NS composed of sorbitan monopalmitate (Span 40) or sorbitan monostearate (Span 60) were prepared through the thin film hydration (TFH) and the ethanol injection (EI) methods. The formulations were subsequently characterized for their physico-chemical and functional properties. Vesicles prepared through TFH showed higher average sizes than the corresponding formulations obtained by EI. All the vesicles presented adequate encapsulation efficiency and a negative ζ potential, which assured good stability during the storage period (except for LP-SPC). Formulations prepared with TFH showed a more prolonged AZT release than those prepared through EI, due to their lower surface area and multilamellar structure, as confirmed by atomic force microscopy nanomechanical characterization. Finally, among all the formulations, NS-Span 40-TFH and LP-EPC-TFH allowed the highest drug accumulation in the skin, retained the antimicrobial activity and did not alter fibroblast metabolism and viability. Overall, they could ensure to minimize the dosing and the administration frequency, thus representing promising candidates for the treatment of bacterial skin infections and acne.

1. Introduction

In the last decade, the incidence of bacterial skin infections has been increasing at an alarming pace, establishing an important clinical and financial burden to health care systems [1]. The invasion of bacteria, such as *Staphylococcus aureus*, *Cutibacterium acnes* (formerly known as *Propionibacterium acnes*), *Staphylococcus epidermidis* and *Streptococcus pyogenes*, is the main cause of skin infections, which can be classified as localized superficial infections, like erysipelas, impetigo, acne folliculitis, rosacea, infected eczema, and deep tissue infections, such as cellulitis [2]. Among these infections, acne vulgaris is considered one of the most common skin diseases encountered worldwide, particularly affecting younger people [3]. Although it is not considered a typical infectious disease, it is characterized by an evident overgrowth of bacteria, like *C. acnes*, *S. aureus* and *S. epidermidis* [4–6]. *C. acnes* overgrowth triggers innate immune system activation, leading to cutaneous inflammation, follicular hyperkeratinization, lipogenesis, microcomedogenesis, and skin lesions of various morphologies, ranging from comedones, papules, and pustules to nodules and cysts [7].

An important aspect linked to skin bacterial infections concerns the alarming global spread of multidrug-resistant strains, which makes these pathologies difficult to treat, posing further a global threat to public health [8]. Particularly, the abuse or the misuse of antibiotics has contributed to the diffusion of increasing number of drug-resistant *S. aureus* and *C. acnes* strains, limiting treatment success [9].

Currently, topical administration of antimicrobial molecules through conventional dosage forms (such as creams, ointments, gels, or sprays) represents the first approach for the treatment of skin bacterial

* Corresponding author.
E-mail addresses: angela.abruzzo2@unibo.it (A. Abruzzo), rossella.pucci@studio.unibo.it (R. Pucci), provvidenza.abruzzo2@unibo.it (P.M. Abruzzo), silvia.canaider@unibo.it (S. Canaider), carola.parolin@unibo.it (C. Parolin), b.vitali@unibo.it (B. Vitali), francesco.valle@cnr.it (F. Valle), marco.brucale@cnr.it (M. Brucale), teresa.cerchiara2@unibo.it (T. Cerchiara), barbara.luppi@unibo.it (B. Luppi), federica.bigucci@unibo.it (F. Bigucci).

https://doi.org/10.1016/j.ejpb.2024.114233
Received 11 December 2023; Received in revised form 8 February 2024; Accepted 19 February 2024
Available online 20 February 2024

infections, owing largely to its advantage of minimizing drug systemic exposure. However, topical formulations present some drawbacks related to the difficulty to reach adequate drug concentration at the infected site [10]. This in turns requires multiple administrations, thus impairing patient compliance and worsening the antibiotic-resistance phenomenon [11]. The encapsulation of anti-infective agents into nanocarriers can represent an innovative approach useful to tackle the mentioned problems as well as to improve the therapeutic efficacy of anti-infective agents. In particular, peculiar characteristics of these drug delivery systems, like carrier size and surface charge, controlled release, the ability to interact with the main components of the skin, can allow to dramatically improve skin accumulation of the delivered drugs [12]. Additionally, multiple interactions of the nanosystems with the bacterial cell can promote cell wall and membrane disruption, membrane fusion and damage of bacterial intracellular components, thus improving the antimicrobial activity [13].

Azithromycin (AZT) is a macrolide antibiotic targeting the 50S bacterial ribosomal subunit, which inhibits protein synthesis, thus hindering the growth of bacteria [14]. Although AZT is mainly administered by oral and intravenous route, for the treatment of skin infections topical antibiotic therapy is crucial to avoid high dose and side effects [15]. Until now, only few papers have reported the use of nanosystems containing AZT for the topical treatment of skin infections. Particularly, Rukavina and colleagues [16] developed different types of AZT-loaded liposomes (conventional, deformable and containing PEG) to locally treat skin infections caused by methicillin-resistant *S. aureus* (MRSA) strains and demonstrated that all the prepared liposomes retained the drug inside the skin more efficiently than the control. Our recent study reported the preparation of AZT based microemulsions, which were able to guarantee a prolonged drug release and to promote drug accumulation inside the porcine skin [17]. In the current study, for the first time two different types of AZT-loaded vesicles, i.e., liposomes and niosomes (LP and NS) are proposed as useful nanocarriers for the treatment of skin bacterial infections and acne. Furthermore, to the best of our knowledge, this is the first study in which AZT-loaded LP and NS were prepared with different excipients by employing two different manufacturing methods (thin film hydration and ethanol injection) allowing to evaluate the influence of formulation and process factors on the physico-chemical and functional properties of the final products.

LP and NS are vesicles formed by self-assembly of phospholipids and non-ionic surfactants, respectively, which both present the ability to encapsulate hydrophilic and hydrophobic drugs [18,19]. LP also possess the unique property of being biocompatible since their lipid bilayer structure mimics cell membranes and allows fusion with bacterial membranes [20]. However, one of the main limitation of LP regards their chemical instability linked to phospholipid hydrolysis or oxidation [21]. On the other hand, NS are generally characterized by higher chemical stability and longer shelf-life, intrinsic skin penetration enhancing properties and lower costs due to the availability of ingredients with reasonable cost compared to phospholipids [21].

Briefly, the main steps of this work were: (1) to prepare LP and NS with different excipients through the thin film hydration and ethanol injection methods; (2) to characterize them in terms of size, polydispersity index, ζ potential, encapsulation efficiency, morphology, nanomechanics and stability; (3) to investigate LP and NS ability to release the drug and to promote its accumulation within porcine skin; (4) to select the best formulations and to evaluate their antimicrobial activity and safety on fibroblast cells.

2. Materials

L-α-phosphatidylcholine from egg yolk (EPC, purity = 80.1 % of L-α-phosphatidylcholine), sorbitan monostearate (Span 60), cholesterol (Chol), L-cysteine, azithromycin dihydrate (AZT), erythrosine B and all the solvents were obtained from Sigma-Aldrich (Milan, Italy). Phospholipon 90G from soybean lecithin (SPC, containing not less than 94 % L-α-phosphatidylcholine) was a kind gift from LIPON GmbH (Ludwigshafen, Germany). Sorbitan monopalmitate (Span 40) was purchased from Fluka (Milan, Italy). Phosphate buffer at pH 7.4 (PBS) was composed of 2.38 g/L $Na_2HPO_4 \times 12\ H_2O$, 0.19 g/L KH_2PO_4 and 8.00 g/L NaCl. Ultrapure water (18.2 MW cm) was obtained by means of a MilliQ apparatus by Millipore (Milford, MA, USA). Human primary fibroblast cells (NIGMS Human Genetic Cell Repository at the Coriell Institute for Medical, Camden, New Jersey, USA #GM08402) were used for cell viability analysis and for metabolic activity measurement using the Resazurin Cell Viability Assay Kit (alamarBlue™) (Biotium, Fremont, CA, USA). Dulbecco's Modified Eagle's Medium-4.5 g/L of glucose (H-DMEM) (Incorporated Corning, NY, USA) supplemented with 10 % Fetal Bovine Serum (FBS; Gibco, Waltham, MA, USA) and antibiotics (1 % Penicillin-Streptomycin Solution; Thermo-Fisher Scientific, Waltham, MA, USA) was used as standard medium for fibroblast cell culture.

2.1. Preparation of liposomes and niosomes

2.1.1. Thin film hydration (TFH) method

Unloaded and loaded liposomes (LP) and niosomes (NS) were prepared using the thin film hydration (TFH) method as described elsewhere [22] with some modifications. For LP preparation, EPC (70 mg) or SPC (70 mg) and Chol (30 mg) were dissolved in a mixture of $CHCl_3$-CH_3OH (5 mL, 9:1 v/v) in a round-bottomed flask. The organic phase was subsequently evaporated using a rotary evaporator (Buchi Rotavapor R-200, Flawil, Switzerland) operated under reduced pressure (80 mbar) at 60 °C for 90 min. The dried thin lipid film formed on the inner wall of the flask was hydrated with 10 mL of PBS (pH 7.4) by rotating the flask at 210 rpm for 1 h. Later, the obtained milky suspension was extruded through a polycarbonate membrane with a pore size of 100 nm (LiposoFast manual syringe extruder, Avestin Europe GmbH, Mannheim, Germany). Fifteen cycles of extrusion were performed in order to reduce and homogenize vesicle size [23]. For NS preparation, the same mentioned procedure was conducted by replacing phosphatidylcholine with a same amount of surfactant (Span 40 or Span 60).

For the preparation of loaded vesicles, AZT was solubilized in the organic phase obtaining a final drug concentration of 3 mg/mL. The different formulations were named according to their composition as follows: LP-EPC-TFH, LP-SPC-TFH, NS-Span 40-TFH, NS-Span 60-TFH.

2.1.2. Ethanol injection method (EI)

For vesicle preparation through the ethanol injection method, an appropriate weighed amount of EPC, SPC, Span 40 or Span 60 (70 mg) in combination with Chol (30 mg) was dissolved in 5 mL of ethanol 96 %. Then, this solution was injected with a syringe at a flow of 1 mL/min into 10 mL of PBS, under continuous stirring at 400 rpm. After 20 min, ethanol was removed by means of rotary evaporation under vacuum at 60 °C for 10 min with stirring at 210 rpm. The different formulations were named according to their composition as follows: LP-EPC-EI, LP-SPC-EI, NS-Span 40-EI, NS-Span 60-EI.

2.2. Determination of vesicle size, polidispersity index (PDI) and ζ potential

The prepared vesicles were characterized in terms of size, polydispersity index (PDI) and ζ potential. Particle size and PDI were measured at 25 °C by photon correlation spectroscopy (PCS) using a Brookhaven 90-PLUS instrument (Brookhaven Instruments Corp., Holtsville, NY, USA) with an He-Ne laser beam at a wavelength of 532 nm (scattering angle of 90°). For measurements, vesicle suspensions were dispersed in ultrapure water (18.2 MW cm, MilliQ apparatus by Millipore, Milford, MA, USA) with a dilution of 1:1000 (v/v). ζ potential measurements were carried out at 25 °C on a Malvern Zetasizer 3000 HS instrument (Malvern Panalytical Ltd., Malvern, UK) after the same dilution.

2.3. Determination of encapsulation efficiency

To quantify the amount of AZT not incorporated into the vesicles, three different techniques were employed: (1) dialysis, (2) centrifugation, (3) and filtration through Vivaspin tubes [24]. For the first technique, a method previously described [25] with some modification was followed. Specifically, 0.5 mL of the vesicle suspensions were placed inside a Visking Tubo Dialysis membrane (Medicell International Ltd., London, UK) with a cut-off size of 14,000 Dalton. The tube was then immersed into 50 mL of PBS (external phase) and kept at 25 °C under stirring at 100 rpm. After 2 h, 4 h, 6 h and 24 h, aliquots of the external phase were collected and analyzed through high-performance liquid chromatography (HPLC) [17] to determine free AZT. In the case of the second technique, vesicles suspensions were centrifuged at 15,000 rpm (ALC 4239R centrifuge; Milan, Italy) at +4 °C for 1 h; subsequently the supernatant was collected and analyzed through HPLC in order to quantify the amount of non-entrapped drug. For the third technique, vesicle suspensions were centrifuged at 5000 rpm and 25 °C for 30 min using a Vivaspin 500 centrifugal concentrator (Sartorius, Milan, Italy, MW cut off = 5,000 Da) and the resultant filtrate was analyzed through HPLC.

HPLC determination of AZT was carried out following the method previously reported [17], by using a chromatographic system based on a Shimadzu (Milan, Italy) LC-10ATVP chromatographic pump and a Shimadzu SPD-10AVP UV–vis detector set at 215 nm. The column was a Phenomenex (Torrance, CA, USA) Kinetex (150 mm × 4.6 mm I.D., 5 mm) coupled to a Phenomenex (Torrance, CA, USA) Security Guard C18 guard cartridge (4 mm × 3.0 mm I.D., 5 mm). The mobile phase was prepared by mixing a buffer (KH_2PO_4 0.01 M adjusted at the pH 7.5 with 10 M KOH) with methanol and acetonitrile (10/50/40, v/v) and a flux rate of 0.8 mL/min. Solutions of AZT in methanol at drug concentrations ranging from 13 μg/mL to 400 μg/mL were analysed to obtain a standard curve (R^2 = 0.9964). For *in vitro* drug release and permeation/retention results, another calibration curve of AZT was obtained, by using AZT solution in PBS pH 7.4/ ethanol (80:20, v/v) with drug concentrations ranging from 0.5 μg/mL to 50 μg/mL (R^2 = 0.9943).

The EE % was calculated using the following equation:

$$EE\% = \frac{(\text{Total amount of AZT} - \text{Amount in the external phase/supernatant/filtrate}) \times 100}{\text{Total amount of AZT}}$$

2.4. Morphology and nanomechanics

Single-particle quantitative morphometry and nanomechanical characterization of LP and NS obtained via TFH and EI methods were performed as described elsewhere [26,27]. Briefly, samples were deposited on a substrate having a controlled surface charge density; upon adhesion, vesicles deform into oblate spheroids whose surface contact angle is proportional to their mechanical stiffness. Atomic force microscopy (AFM) was then employed to measure several hundred vesicles for each sample; quantitative morphometry then allowed us to reconstruct the diameter and surface contact angle of each individual vesicle and to pool them into representative size and stiffness distributions.

AFM experiments were performed in liquid at RT on a Bruker Multimode8 operated in Peakforce mode and equipped with a Nanoscope V controller using Bruker ScanAsyst FluidPlus probes (triangular cantilever, nominal tip curvature radius 2–12 nm, nominal spring constant 0.7 N/m) calibrated with the thermal noise method. A 10 μl-droplet of the sample was deposited on a PLL-functionalized glass slide prepared as described elsewhere [28] and left to adsorb for 30 min at 4 °C, then inserted in the AFM fluid cell. Applied force was kept under 400 pN to minimize vesicle damage during scanning. Images were analyzed with Gwyddion 2.53 [29] and custom Python scripts as described elsewhere [26].

2.5. In vitro drug release studies

AZT release from vesicle suspensions was assessed through a Franz cell diffusion system under sink conditions using cellulose filter (MF-Millipore Membrane, mixed cellulose esters, pore size = 0.22 μm) and a heating circulator set to 32 ± 1.0 °C [30]. Specifically, a Franz-type static glass diffusion cell (15 mm jacketed cell with a flat ground joint and clear glass with a 12 mL receptor volume; diffusion surface area = 1.77 cm^2), equipped with a V6A Stirrer (PermeGear Inc., Hellertown, PA, USA) was used. A fixed amount of vesicle suspension (0.5 mL) was introduced in the donor compartment, whereas the receiver one was filled with PBS/ethanol mixture (80:20, *v/v*), maintained at 32 ± 1.0 °C by means of a surrounding jacket. At 0.5, 1, 2, 3, 4, 5 and 6 h, samples (0.2 mL) were withdrawn from the receiver compartment, replaced with fresh medium and analysed using HPLC. A control sample based on a mixture of ethanol and water (60:40, v/v) containing an equivalent amount of AZT was also tested. Results are shown as cumulative drug amount released (expressed as fractional amount Mt/M0, where Mt represents the amount of AZT released at each time and M0 the total AZT mass loaded into vesicle suspensions or control) plotted as a function of time.

2.6. Vesicle physical stability

The physical stability of the prepared vesicles was monitored during a storage period of 180 days at 4–8 °C or 25 °C. At determined time intervals (7, 14, 30, 60, 90, 150 and 180 days), aliquots of vesicle suspensions were diluted in ultrapure water as described in Section 2.2, and changes in vesicle size and PDI were monitored using PCS. Appearance of sedimentation processes was monitored during the storage period.

2.7. In vitro skin Permeation/Retention studies

For the determination of AZT ability to diffuse or to be retained inside the skin, *in vitro* studies were performed by employing the porcine ear skin isolated as previously described [17]. For the experiments, the skin was mounted in the Franz diffusion cells with the stratum corneum side facing upwards. The receptor chamber was filled with 12 mL of PBS and ethanol (80:20, v/v) and maintained at 32 ± 1.0 °C. At time zero 0.5 mL of the formulation were placed in the donor chamber and at fixed time intervals until 24 h, samples (0.2 mL) were collected from the receiver chamber, replaced with the same amount of fresh medium and analysed using HPLC. A control sample based on a mixture of ethanol and water (60:40, v/v) containing an equivalent amount of AZT was also tested.

For determining skin retention of AZT from developed LP and NS, after 24 h, the residual formulations contained in the donor compartment were wiped off and the skin surface was carefully rinsed with methanol (0.5 mL). Both fractions were diluted in methanol and analysed through HPLC to determine the non-penetrated drug (AZT in the donor compartment). Subsequently, the skin was gently removed, cut into very small pieces and placed in methanol (5 mL) for 5 h under

magnetic stirrer (300 rpm) to extract the drug. Skin was then withdrawn and the solution was centrifuged at 14,500 rpm for 20 min and analysed through HPLC to determine AZT amount retained within the skin. The results of *in vitro* permeation/retention studies are shown as percentage of drug amount inside the donor compartment, the skin and the receptor chamber.

2.8. Antimicrobial and antibiofilm activity

The antimicrobial activity of AZT-loaded vesicles and AZT (ethanol and water 60:40, v/v containing an equivalent amount of AZT) was determined against *S. aureus* and *C. acnes* strains, belonging to the collection of the Department of Pharmacy and Biotechnology, University of Bologna. *S. aureus* ATCC 29213, *S. aureus* strain #7 (resistant to beta-lactams, fluoroquinolones, ansamycins), *S. aureus* strain #83 (resistant to betalactams, fluoroquinolones) and *S. aureus* strain #88 (resistant to aminoglycosides) were routinely grown in nutrient broth (NB, Difco, Detroit. MI), at 37 °C [17,31]. *C. acnes* BC106 was routinely grown in de Man, Rogosa, Sharpe medium (MRS, Difco) supplemented with 0.05 % L-cysteine, at 37 °C in anaerobic jars containing GasPak EZ (Becton, Dickinson and Co., Milan, Italy).

To assess minimal inhibitory concentrations (MIC, corresponding to the lowest concentration of antimicrobial agent that completely inhibits growth of the organism in the microdilution wells as detected by the unaided eye) of AZT and AZT-loaded vesicles, a microdilution assay was carried out on a 96-well plate, following NCCLS standard guidelines [32]. Briefly, AZT solution and vesicle suspensions were 2-fold serially diluted in appropriate culture medium and added to bacterial suspensions. AZT tested concentrations were in the range 0.05–30 μg/mL. MIC values were determined after 24 h of incubation. In order to determine whether the formulations retained their antimicrobial activity over the storage period, MIC was also determined after that AZT-loaded vesicles were stored for 180 days at +4–8 °C.

The antibiofim activity was tested on the same bacterial strains following the procedure reported in our previous study [31] with slight modifications. Briefly, bacterial suspensions were inoculated in flat bottom 96-well plates in the presence of AZT-loaded vesicles at concentrations equal to MIC and 2 × MIC and allowed to grow for 72 h. Unloaded NS and LP were also tested at the same dilutions of the corresponding AZT-loaded vesicles. Biofilm formation was assessed and quantified by crystal violet staining and reading OD595 by using an EnSpire Multimode Plate Reader (PerkinElmer Inc., Waltham, MA). Inhibition of bacterial biofilm formation was expressed in percentage relative to the control wells, based on the average of four biological replicates [31].

2.9. Resazurin-based metabolic assay

The impact of the AZT-loaded formulations on cell functionality was assessed by measuring metabolic activity in human primary fibroblasts using the Resazurin Cell Viability Assay Kit. Resazurin is a redox indicator used to evaluate metabolic function and cellular health [33]. When this compound is added to standard culture medium, metabolically active cells reduce the Resazurin non-fluorescent dye to a highly fluorescent molecule, Resorufin. Fibroblast cells were seeded at density of 3000 cells/cm^2 in a 96-well plate (Corning Incorporated, Corning, NY, USA), in standard medium and cultured in standard conditions at 37 °C with 5 % carbon dioxide (CO_2) in a humidified atmosphere. After 24 h, cells were treated with the AZT solution (in ethanol and water, 60:40, v/v) at different concentrations (75, 30, 8, or 4 μg/mL) or with LP or NS containing the same AZT concentrations (obtained from the starting suspensions after adequate dilution in PBS). Untreated cells (CTR, cells cultured in standard medium) were used as a positive metabolic control. Formulations were added to the standard culture medium containing 10 % of Resazurin compound. Resorufin fluorescence was measured 24 h after treatment by employing the Wallac 1420 Victor2 Multilabel Counter (Perkin Elmer, Waltham, MA, USA) at 590 nm, using an excitation wavelength of 560 nm. Each condition was assayed in triplicate; negative controls (standard medium with 10 % of Resazurin with or without formulations) and the completely reduced Resazurin (100 % reduced Resazurin) were included. The 100 % reduced Resazurin was obtained by autoclaving at 121 °C the standard medium with 10 % of Resazurin for 15 min. Metabolic activity was expressed as a percentage of Resazurin reduction according to the following formula:

% Resazurin reduction: = (FI 590 of test agent- FI 590 of negative control)/(FI 590 of 100 % reduced Resazurin-FI 590 negative control) × 100 where FI is the fluorescence intensity.

2.10. Cell viability

Human primary fibroblast cells were seeded in a 6-well plate (Corning Incorporated, Corning, NY, USA) at a density of 5000 cells/cm^2 and were maintained for 24 h in standard conditions. Then, cells were treated for 24 h with AZT solution (in ethanol and water, 60:40, v/v) (30 μg/mL) or with LP or NS containing the same AZT concentration (obtained from the starting suspensions after adequate dilution in PBS). Untreated cells (CTR, cells cultured in standard medium) were used as a positive viability control. Cell viability was assessed by manual cell count using erythrosine B, a dye which stained in red dead cells [34]. Briefly, cells were detached by trypsin–EDTA and were resuspended in a medium containing 50 % erythrosine B 0.2 % in PBS. Unstained viable cells and red-stained dead cells were counted using the Neubauer hemocytometer (BRAND GmbH, Wertheim, Germany) under a light microscope Leica Labovert FS inverted Microscope (Leica Microsystems, Wetzlar, Germany). The number of viable and dead cells were calculated according to the manufacturer's instructions; cell viability was obtained by calculating the percentage of living cells compared to the total number of cells.

2.11. Statistical analysis

All experiments were done in triplicate, except for *in vitro* skin permeation/retention studies which were performed in five replicas. Microbiological tests were done at least in four replicas. Results are expressed as mean ± SD. *t*-test was used to determine statistical significance, one-way ANOVA and Dunnett's multiple comparison test were applied to biofilm inhibition data. The criterion for statistical significance was $p < 0.05$.

3. Results and discussion

3.1. Preparation of LP and NS

The objective of this work was to develop new nano-sized drug delivery systems useful to be employed for the treatment of bacterial skin infections and acne. With this aim, firstly we prepared AZT-loaded LP and NS by employing two manufacturing methods (TFH and EI) and different excipients. Subsequently, we investigated the impact of the composition and the preparation method on the physico-chemical as well as the functional properties of the developed vesicles. TFH method is the main technique used for the preparation of LP and NS and generally it allows to obtain large multilamellar vesicles which can be reduced in size by a post-manufacturing step. This method is particularly employed for the loading of hydrophobic molecules, thanks to the presence of several phospholipids/surfactants-based bilayers able to include lipophilic drugs [35]. However, the need of several steps, which negatively impair the potential industrial scale process, combined to the use of organic solvents has reduced the interest of researchers towards this technique, shifting the attention on alternative preparation

Table 1
Size, PDI and ζ potential values of unloaded and loaded LP and NS.

	Size (nm)		PDI		ζ potential (mV)	
	Unloaded	Loaded	Unloaded	Loaded	Unloaded	Loaded
LP-EPC-TFH	363.1 ± 21.7	456.7 ± 2.7	0.310 ± 0.017	0.315 ± 0.020	−66.5 ± 1.0	−61.8 ± 1.7
LP-SPC-TFH	249.2 ± 22.9	311.7 ± 10.0	0.293 ± 0.015	0.311 ± 0.014	−51.1 ± 0.2	−52.0 ± 1.9
LP-EPC-EI	180.2 ± 4.2	247.5 ± 1.3	0.154 ± 0.090	0.138 ± 0.089	−56.7 ± 1.4	−48.9 ± 0.1
LP-SPC-EI	151.6 ± 3.3	176.9 ± 3.4	0.106 ± 0.011	0.153 ± 0.012	−48.9 ± 0.7	−45.1 ± 0.9
NS-Span 40-TFH	549.8 ± 49.8	676.3 ± 21.1	0.315 ± 0.009	0.293 ± 0.053	−78.0 ± 1.8	−66.2 ± 2.1
NS-Span 60-TFH	591.4 ± 55.1	757.7 ± 28.2	0.224 ± 0.047	0.307 ± 0.044	−67.5 ± 3.5	−58.2 ± 0.8
NS-Span 40-EI	231.3 ± 5.9	299.6 ± 6.5	0.137 ± 0.019	0.175 ± 0.025	−67.5 ± 0.8	−60.3 ± 0.7
NS-Span 60-EI	280.9 ± 1.0	329.0 ± 8.1	0.136 ± 0.024	0.237 ± 0.011	−52.8 ± 0.6	−45.4 ± 0.2

methods. Among these, the EI method is characterized by relevant advantages such as simplicity, absence of potentially unsafe solvents, and easy scaling-up; moreover, it allows preparing vesicles with low size and homogenous distribution without the need for post-manufacturing size reduction steps and with high reproducibility. Another advantage of EI with respect to TFH is the time required for obtaining vesicles since the preparation procedure takes minutes in the case of EI, and different hours in the case of TFH. On the other hand, different parameters used with the EI method, such the flow rate, the lipid concentration, as well as the stirring rate, can affect vesicle properties [36]. Furthermore, some other drawbacks, related to the difficulty of removing ethanol specifically after azeotrope formation, could negatively affect the method efficacy, thus limiting its potential application. Another limitation is linked to the solubility of lipids/surfactants and drugs, together with their possible degradation in ethanol, which influence the vesicle formation and the encapsulation efficiency [36].

In addition to the preparative methods, the influence of using different excipients on the final functional properties of vesicles was also investigated. Specifically, LP were developed by using EPC or SPC, which differ in terms of source and purity as well. In fact, EPC and SPC are phosphatidylcholines derived from egg yolk and soybean, respectively; EPC presented a purity of 80.1 %, conversely SPC was based on not less than 94 % L-α-phosphatidylcholine (as indicated in manufacturer specifications for the employed batches). Our previous works reported the use of these types of phosphatidylcholines for the design of liposomes able to deliver drugs or biosurfactants [23,31,37]. Instead, Span 40 and Span 60 were selected for NS preparation. Span 40 and Span 60 present different length of alkyl chain (C16 and C18 for Span 40 and Span 60, respectively), transition temperature (42 °C and 53 °C for Span 40 and Span 60, respectively), and HLB (7.6 and 4.7 for Span 40 and Span 60, respectively). It has been reported that all these factors contributed to the formation of NS with different properties in terms of size, encapsulation efficiency and drug release [18]. Finally, Chol was added since it has known that it can promote the packing of lipid chains and bilayer formation, and consequently influence the drug release as well as vesicle stability [35].

3.2. Determination of vesicle size, polidispersity index (PDI) and ζ potential

The measurement of vesicle size and PDI represents an important evaluation in the case of vesicles intended for skin application. In fact, previous research reported that small vesicles could penetrate deeper into the skin layers than the larger ones. Particularly, vesicles with an average size >600 nm were not able to penetrate in deep layers of the skin and mostly remained on the surface of the stratum corneum, forming a layer of lipid, while vesicles with an average diameter of 300 nm could penetrate deeper into skin layers [38]. Vesicle size can also influence drug release and consequently its diffusion/retention inside the skin; generally, larger particles present a reduced surface area, which results in a reduced diffusion of the drug out of the system [39]. Simultaneously PDI determination is fundamental to estimate the sample homogeneity. In general, PDI values below 0.3 are representative of homogenous samples [40].

Table 1 shows the size and PDI values of LP and NS with (loaded) or without drug (unloaded).

Vesicles obtained through the TFH method showed larger average sizes than those obtained from the same formulations via the EI method ($p < 0.05$). In particular, vesicles obtained through TFH followed by the French Press step showed average sizes ranging from 249.2 nm to 757.7 nm and PDI values from 0.224 to 0.315. The EI method provided vesicles with size ranging from 151.6 nm to 329.0 nm and PDI values from 0.106 to 0.237. This result can be correlated to the intrinsic mechanisms of vesicle formation, involved in the different employed methods. As reported in literature, the TFH method usually yields large multilamellar vesicles, and their successive extrusion through the French Press provides a reduction in size and PDI [41,42]. It is worth pointing out that after this this step, extruded vesicles can still be larger than the filter's pore size, due to their reversible elastic deformation upon extrusion as previously reported [39]. On the other hand, the EI method leads to the formation of smaller unilamellar vesicles following the addition of ethanol solution inside the aqueous phase [42] (see Section 3.4).

Regarding LP composition, it was possible to highlight that vesicles composed of EPC were characterized by a larger size with respect to vesicles based on SPC ($p < 0.05$). This behaviour can be linked to the lower purity (as previously indicated) of EPC, which could favour the formation of larger vesicles than SPC. Instead, as regards NS, the employment of Span 40 led to the formation of vesicles with lower size with respect to Span 60 ($p < 0.05$). This result can be attributed to the different chain length of surfactants: Span 40, which possess a C16 alkyl chain determined the formation of smaller vesicles than Span 60 composed of C18 alkyl chain, according to previous studies [43,44]. Additionally, by comparing LP and NS it was possible to observe that NS were larger in size with respect to LP ($p < 0.05$), probably due to the different self-assembling of phosphatidylcholines and anionic surfactants and to the presence of a larger aqueous compartment in the case of NS. Finally, unloaded vesicles presented a lower size than the loaded ones ($p < 0.05$), as a consequence of the presence of drug molecules inside the structures which determined an increase in their dimension [25,45,46].

Another important property of LP and NS is the superficial charge, which was determined through the measurement of ζ potential. It has been reported that ζ potential can impact on the vesicle ability to be retained inside the skin as well as on their stability. Particularly, Gillet and co-workers reported that negatively charged nanosystems can greatly accumulated inside the skin with respect to neutral or positively charges ones [47]. Moreover, it has been widely recognized that ζ potential values lower than −30 mV or higher than +30 mV can limit vesicle aggregation, thus improving their stability [48]. Formulations obtained in this study showed ζ potential values which varied from −78 mV to −45 mV. The negative charge can be correlated to the presence of hydroxylic groups of cholesterol and surfactants (in the case of NS) and phosphate groups of phosphatidylcholine (in the case of LP), in agreement with previous findings [25,49,50]. Generally, vesicles obtained through TFH presented a more evident negative surface in comparison to vesicles obtained through EI, probably due to the different

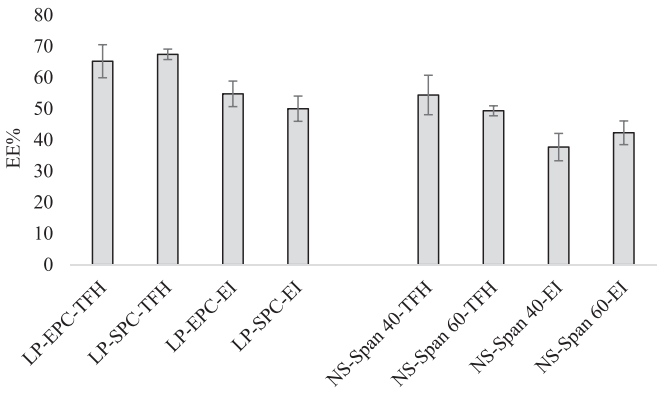

Fig. 1. Encapsulation efficiency (EE%) values obtained for the different formulations.

organization of hydrophilic portion in the bilayers during the production steps. Furthermore, LP composed of EPC showed a more negative ζ potential value ($p < 0.05$) with respect to vesicles based on SPC, due to the presence of fatty acids in the composition of EPC able to further reduce the surface charge. As regards NS, Span 60 provided the formation of vesicles with a less negative ζ potential values ($p < 0.05$) than Span 40, as consequence of the lower hydrophilic properties of Span 60 (HLB Span 40 = 7.6, HLB Span 60 = 4.7) which, according to other previous results, decreased the surface free energy of the surfactant [51].

Finally, in the presence of loaded vesicles an increase in ζ potential value was observed with respect to the unloaded ones ($p < 0.05$), probably due to the presence of positive charges of AZT (pKa = 8.5) at the experimental pH (7.4), which led to the formation of vesicles with a less negative surface charge [52].

3.3. Determination of encapsulation efficiency

Encapsulation efficiency (EE%) is a key characterization parameter that demonstrates the vesicle's capacity for drug encapsulation. The encapsulation efficiency was measured by exploiting three different techniques. Dialysis method allowed to measure the non-encapsulated AZT amount able to diffuse through the membrane and reach the external phase. Aliquots of the external phase were withdrawn after 2, 4, 6 and 24 h and results demonstrated that the AZT amount in the external phase did not change over the time. This method permitted to obtain results after 2 h by consuming only a small amount of vesicle suspensions. The second method based on centrifugation provided the isolation of a supernatant consisting of free AZT, at the expense of using a higher amount of vesicle suspension (minimum of 10 mL with our instrumentation) with a consequent wastefulness of excipients and drug. The latter method allowed to isolate the free amount of drug by exploiting the filtration process through Vivaspin tubes; despite the possibility of using a small amount of vesicle suspensions (lower than 500 μl), this method was the most expensive among the three methods used for the determination of encapsulation efficiency because of the tube cost. However, when analysing the same samples with the different methods no differences were observed ($p > 0.05$). Fig. 1 shows the encapsulation efficiency values obtained with dialysis method. Vesicles obtained through TFH method were characterized by higher value of EE% with respect to vesicles obtained through EI ($p < 0.05$), suggesting that their multilamellarity (see Section 3.4) might enhance drug incorporation. However, no significant difference was observed between EPC and SPC-based LP, as well as between Span 40 and Span 60 based NS ($p > 0.05$). Furthermore, LP tendentially allowed the encapsulation of a greater amount of drug with respect to NS ($p < 0.05$). This result can be probably attributed to the pore-formation characteristics in the bilayer of NS, in agreement with previous results [53]. In all cases, the inclusion of AZT inside LP and NS allowed to obtain vesicle suspensions with a final drug concentration equal to 3 mg/mL, thus achieving an increase of drug solubility (AZT solubility in water equal to 0.14 ± 0.02 mg/mL; [17]). The presence of a greater amount in the solubilized form represents an important advantage in order to reach the bioavailability of the drug at the target site and fulfil the therapeutic action [54].

3.4. Morphology and nanomechanics

In order to evaluate vesicle morphology, we performed single-particle AFM morphometric characterization [27] of loaded LP and NS (LP-EPC and NS-Span 40) obtained via both TFH and EI (Fig. 2). Although the resulting diameter distributions are non-normally distributed, comparing their averages ± standard deviations still allows performing a rough comparison between them. NS-Span 40-TFH and LP-EPC-TFH were found to have average diameters of 187 ± 107 and 197 ± 155 nm, while NS-Span 40-EI and LP-EPC-EI showed averages of 107 ± 43 and 100 ± 87 nm. As expected, the size distributions of vesicles obtained via TFH show both larger diameters and higher variances with respect to those prepared by EI. The apparent discrepancy of all distributions being shifted to lower average values with respect to their counterparts listed in Table 1 can be reconciled by considering that geometrical particle sizes as measured via microscopy techniques such as AFM are almost always lower than hydrodynamic particle sizes obtained by PCS techniques. In contrast, we recently showed how, for several different classes of membranous particles, size distributions reconstructed with our AFM-based method are practically coincident

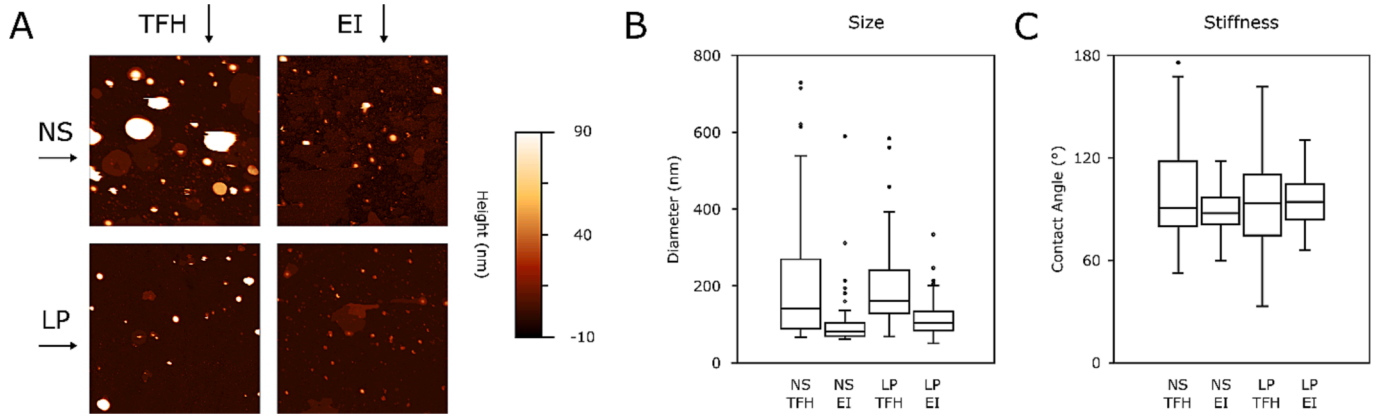

Fig. 2. (A) Representative AFM micrographs of NS-Span 40 (top row) and LP-EPC (bottom row) prepared via TFH (left column) and EI (right column). All images are 5x5 μm. (B) Box plot of vesicle diameters, showing larger sizes and dispersions in TFH samples. (C) Box plot of vesicle contact angles (proportional to mechanical stiffness), showing that TFH samples have similar median values but higher variances with respect to EI samples, suggesting an higher degree of multilamellarity.

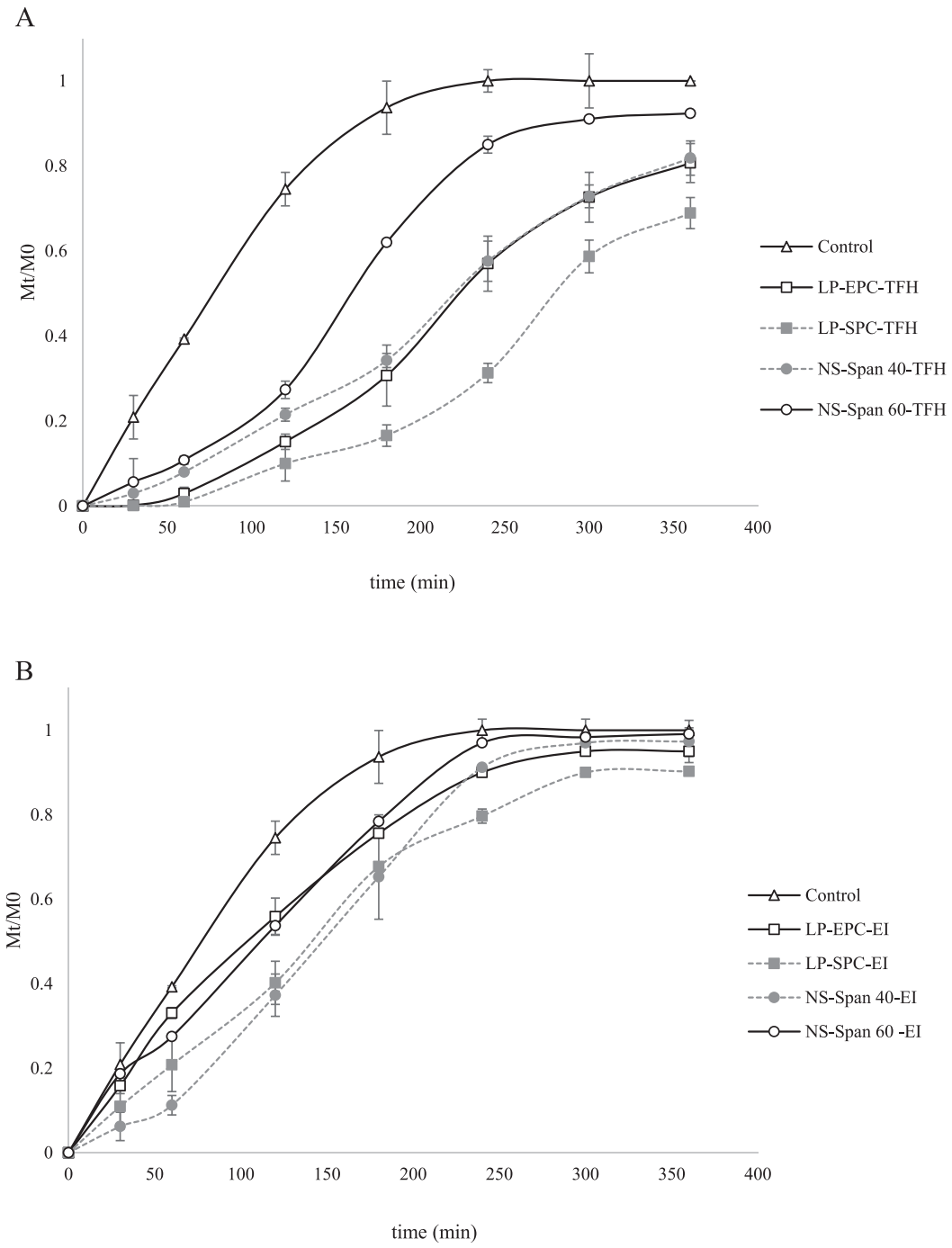

Fig. 3. Cumulative drug amount (expressed as fractional amount Mt/M0, where Mt represents the amount of AZT released at each time and M0 the total AZT mass) released from vesicles obtained through TFH (A) and EI (B) methods and control plotted as a function of time. Data are expressed as means ± SD, n = 3.

with those obtained via cryogenic electron microscopy [28]. In addition, AFM morphometry was used to measure the vesicles' average contact angle (CA), which is representative of their mechanical stiffness [26]. It is well known that multilamellar vesicles display higher mechanical stiffness than their unilamellar equivalents [55]. When compared to EI-derived samples, vesicles obtained via TFH yielded significatively broader CA distributions, even though the main modes of these distributions remained the same as the EI samples. This result suggests that the sharper EI distributions correspond to unilamellar vesicles, while TFH formulations comprise a mix of uni- and multilamellar vesicles, thus resulting in the observed higher variance of mechanical compliances.

3.5. *In vitro drug release studies*

Drug release from the different vesicles can be influenced by several parameters, like the presence of the different bilayers and the drug distribution inside the vesicle structure as well as the vesicle size and composition. Fig. 3A and B show the *in vitro* drug release profiles obtained for the vesicles prepared through TFH and EI methods, respectively, compared with the control sample. Generally, all the developed vesicles determined the release of a lower amount of AZT with respect to the control ($p < 0.05$) over the time. This behaviour is obviously related to the different ability of drug to diffuse from the samples or control towards the receptor compartment. Particularly, in the control AZT was

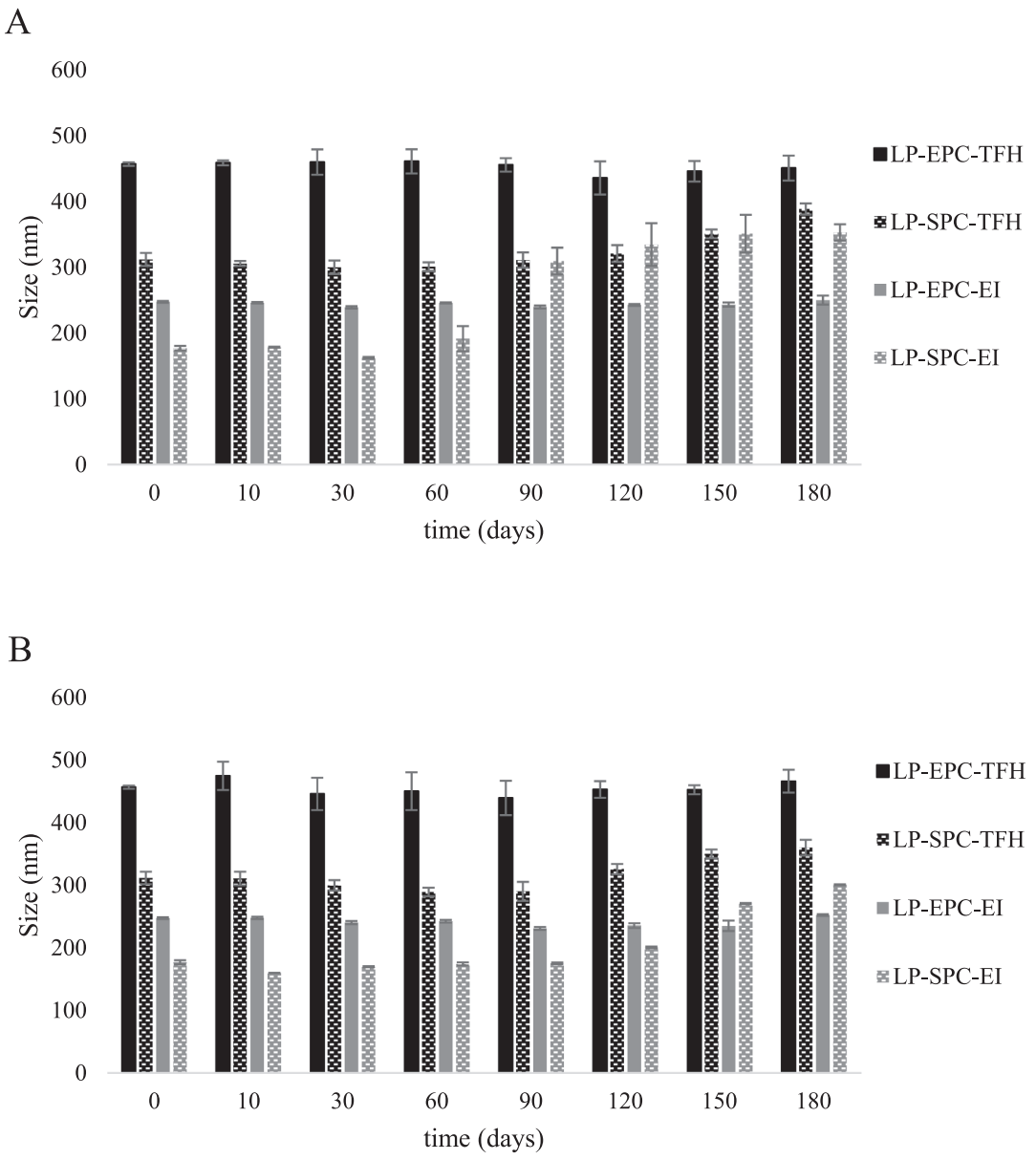

Fig. 4. Size variation of loaded LP during 180 days of storage at +4–8 °C (A) and +25 °C (B). Data are expressed as means ± SD, n = 3.

completely dissolved and rapidly diffused through the membrane, reaching the maximum amount in the receptor compartment after 180 min. On the other side, a controlled release of AZT was obtained in the case of LP and NS; this is strictly linked to the partition steps between the bilayers, to which the drug is subjected before reaching the receptor compartment. Moreover, vesicles obtained through EI method provided the release of a greater amount of AZT over the time with respect to vesicles prepared through TFH method ($p < 0.05$). Specifically, vesicles obtained through EI method allowed to reach the maximum amount of the released drug after 240 min for NS-Span 60 and after 300 min for the other formulations. On the other side, vesicles prepared with TFH method showed a more sustained AZT release over the time, and only in the case of NS-Span 60 the plateau was reached (after 300 min). This result can be correlated to 1) the higher size of vesicles obtained through TFH with respect to the corresponding formulations prepared by EI method, and consequently to their lower surface area able to limit the drug release [39], 2) the higher multilamellarity of vesicles obtained through TFH method, which further limited AZT release; 3) the presence of a lower amount of free drug in vesicle suspension obtained through TFH with respect to than prepared with EI method (EE% of TFH-vesicles > EE% EI-vesicles). However, despite the differences in size between EPC and SPC based LP (size of EPC-LP > SPC-LP) or between Span 40 and Span 60 based NS (Span 60-NS > Span 40-NS), a different trend was observed. As regard LP, the presence of EPC provided the release of a higher amount of drug with respect to SPC ($p < 0.05$), probably due to the presence of impurities in EPC, like fatty acids, which could improve drug solubilization and its release. Furthermore, NS-Span 60 provided the release of a greater amount of drug with respect to NS-Span 40, probably due to the longer alkyl chain length of Span 60 able to promote the drug release [56]. Among all the formulations, NS-Span 40-TFH, LP-EPC-TFH e LP-SPC-TFH guaranteed the most sustained release of AZT over the time. This aspect is of fundamental importance in order to reach adequate local concentration of the drug over the time and to facilitate a prolonged topical therapy [39]. Lastly, these factors could consequently allow to reduce the dosage and the administration frequency, thus finally improving the efficacy of the treatment as well as the patient compliance [57].

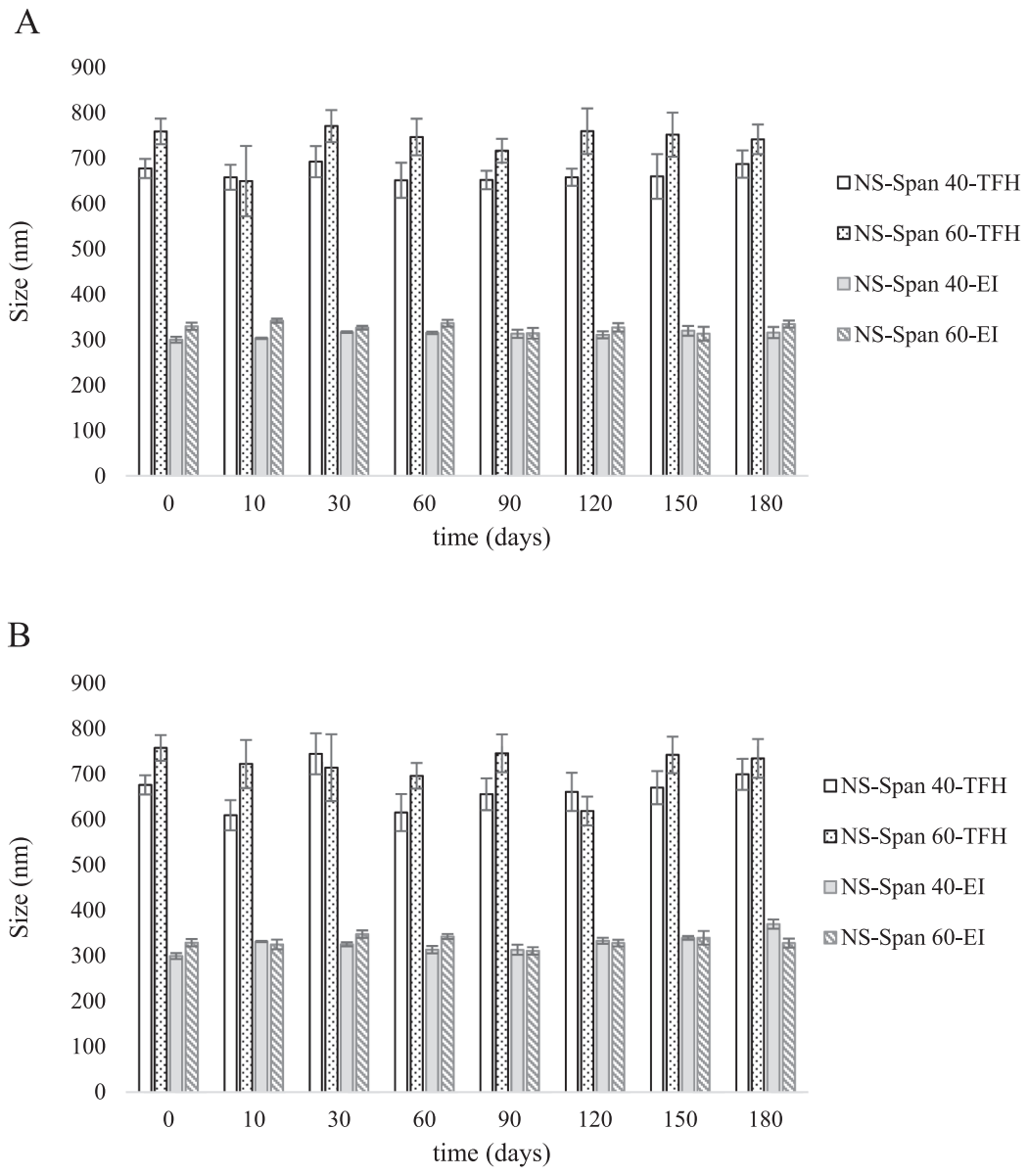

Fig. 5. Size variation of loaded NS during 180 days of storage at +4–8 °C (A) and +25 °C (B). Data are expressed as means ± SD, n = 3.

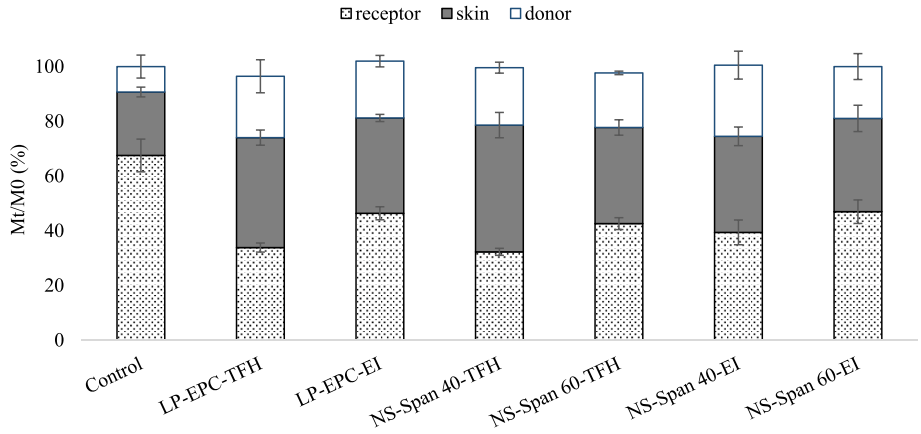

Fig. 6. Percentage amount of AZT in the receptor compartment, within the skin and in the donor compartment obtained after 24 h from the application of control, LP or NS. Data are expressed as means ± SD, n = 5.

3.6. Vesicle physical stability

Stability study was carried out by keeping the formulations at storage conditions (refrigerated temperature and room temperature) for 180 days. The effect of storage on size of LP and NS is reported in Figs. 4 and 5, respectively. For all the developed formulations (with except for LP-SPC), no variation in size and PDI was observed over the storage period (PDI data not shown). The maintenance of vesicle size during the 180 days indicated the good stability of these formulations. Stability was guaranteed by the negative ζ potential values, which favour the electrostatic repulsion and consequently limit vesicle fusion or aggregation. In the case of LP-SPC, after 180 days an increase in size of 25 % and 15 % was observed for LP obtained with the TFH method and stored at +4–8° C and 25 °C, respectively; while for LP-SPC-EI the increase in size was equal to 99 % and 70 % at +4–8 °C and 25 °C, respectively. This result was probably attributed to the process of phospholipid hydrolysis and oxidation which were reported as the main causes of LP instability [58]. Particularly, differently to EPC, which contains free unsaturated fatty acids able to reduce oxidation of phosphatidylcholine [59], SPC presents a high percentage of L-α-phosphatidylcholine (not less than 94 % of L-α-phosphatidylcholine) and probably it was more susceptible to hydrolysis and oxidation than EPC [60]. Furthermore, no significant sedimentation phenomena were observed in all the formulations during the storage period, with except for LP-SPC which presented sedimentation after 120 days of storage. Hence, further studies on LP-SPC were not performed.

3.7. In vitro skin permeation/retention studies

In the field of skin disease treatment, one of the most remarkable challenges is to deliver sufficient concentration of drug to the target site in the skin and minimize at the same time the diffusion of the drug toward the systemic circulation. Hence, *in vitro* skin permeation/retention studies were carried out to evaluate the amount of AZT able to reach the receptor compartment or to be retained inside the skin. This kind of evaluation allows to predict the possibility to maintain the drug inside the skin and therefore to obtain an improvement of the treatment of skin infections.

Several factors, like size, surface charge, composition of the vesicles as well as the drug release behaviour can influence drug retention and diffusion through the skin [38]. Our results demonstrated that after 6 h from LP and NS application, no detectable amount of AZT was measured in the receptor compartment, while the control sample provided the diffusion of 8.79 ± 0.77 % of the total amount of drug. Fig. 6 shows the cumulative amount percentage, obtained after 24 h from the application of the different formulations and the control, in the donor compartment, in the skin and in the receptor compartment. As can be seen, the control sample determined the presence of a greater amount of drug (67.51 ± 5.98 %) in the receptor compartment with respect to the other samples ($p < 0.05$). This result can be attributed to the release behaviour: samples, which determined the release of a greater amount of drug, were able to greatly promote drug diffusion across the skin. For the same reason, in the presence of vesicles obtained through TFH method a lower amount of AZT was found in the receptor compartment with respect to vesicles prepared with EI method ($p < 0.05$). Among all the formulations, LP-EPC-TFH and NS-Span 40-TFH provided the lowest drug permeation after 24 h from the sample application (33.86 ± 4.52 % and 32.29 ± 1.66 %, respectively). This finding is of particular importance considering the need of reducing the drug systemic absorption, which represents a basic requirement for local treatment. In fact, for the treatment of skin diseases, it is more effective and safer to retain drugs deep in the skin than to favour their absorption into the blood circulation. Moreover, in the case of the administration of antibiotic molecules, the possibility of limiting the systemic exposure is another attractive point especially considering the increasing demand of restraining the antimicrobial resistance development.

Table 2
MIC (μg/mL) of free AZT and AZT-loaded vesicles.

Bacterial strain	AZT	LP-EPC-TFH	NS-Span 40-TFH
S. aureus ATCC 29213	1	2	2
S. aureus #7	4	8	15
S. aureus #83	2	8	8
S. aureus #88	2	8	8
C. acnes BC106	0.2	0.5	0.5

As regard drug retention inside the skin, AZT was greatly retained in the presence of all the formulations with respect to the control sample: this finding can be probably related to the release behaviour as well as to the presence of phospholipid or surfactants able to interact with the skin components and consequently to favour drug accumulation [61,62]. Moreover, among all the formulations, LP-EPC-TFH and NS-Span 40-TFH allowed to achieve the highest drug accumulation inside the skin (40.18 ± 3.41 % and 46.32 ± 2.78 %, respectively). This result can be also correlated to the ζ potential values of these formulations (−61.75 ± 1.75 mV e −66.17 ± 2.08 mV, respectively) and was in agreement with previous findings. In fact, it has been recognized that vesicles with a negative ζ potential can improve the retention of drug [47]. Although promising results have been obtained in this study, future studies will be performed in order to evaluate the distribution of the formulations in the pig skin through fluorescence or confocal microscopy and to determine their efficacy on animal models. However, the possibility of reaching an improved drug accumulation inside the skin with the application of vesicle formulations represent an important advantage in the topical treatment of skin infections. In fact, this interesting property can overcome the major limit of topical administration of conventional dosage forms, that is a low drug retention at the infection site. Moreover, the long residence of drug in skin layers is desirable as it can ascertain depot formation, which can prolong drug action [57]. As consequence, all these aspects could permit to reduce drug dosage and administration frequency, thus increasing patient compliance and limiting the risk of antibiotic overuse.

Results obtained from this study revealed that LP-EPC-TFH and NS-Span 40-TFH were able to better localize AZT in the skin and prevent AZT to escape to the receptor fluid and for this reason they were selected for further studies.

3.8. Antimicrobial activity

Free AZT, LP-EPC-TFH and NS-Span 40-TFH were tested towards *S. aureus* and *C. acnes*, as representatives of skin pathogens. For *S. aureus,* a reference strain (ATCC 29213) and antibiotic resistant clinical isolates (strains #7 and #83 are MRSA, strain #88 is resistant to aminoglycosides) were used. MIC values were determined at 24 h by microdilution assay and reported in Table 2.

S. aureus MIC values are in accordance with previously reported data [17,63], confirming a slightly less susceptibility of clinical isolates with respect to reference strain ATCC 29213. When AZT was included in LP-EPC-TFH and NS-Span 40-TFH, two-fold MIC values were registered for *S. aureus* ATCC 29213 and *S. aureus* #7 (only for loaded LP-EPC-TFH), and four-fold MIC values were determined for *S. aureus* #83 and #88 clinical isolates. *C. acnes* BC106 displayed a MIC of 0.2 μg/mL and, even for this bacterium, the formulation of AZT into LP-EPC-TFH and NS-Span 40-TFH vesicles led to increased MIC (two-fold). AZT antimicrobial activity vs *S. aureus* and *C. acnes* was thus retained, although the inclusion of AZT in LP-EPC-TFH and NS-Span 40-TFH determined slightly increased MIC values. This result could be correlated to the *in vitro* release behaviour, in agreement with previous findings [64]. In fact, as previously described, the encapsulation of AZT in LP and NS determined a more sustained drug release than the control and for this reason a low amount of AZT was available to immediately act, thus getting slower their overall antimicrobial activity. Finally, MIC values of

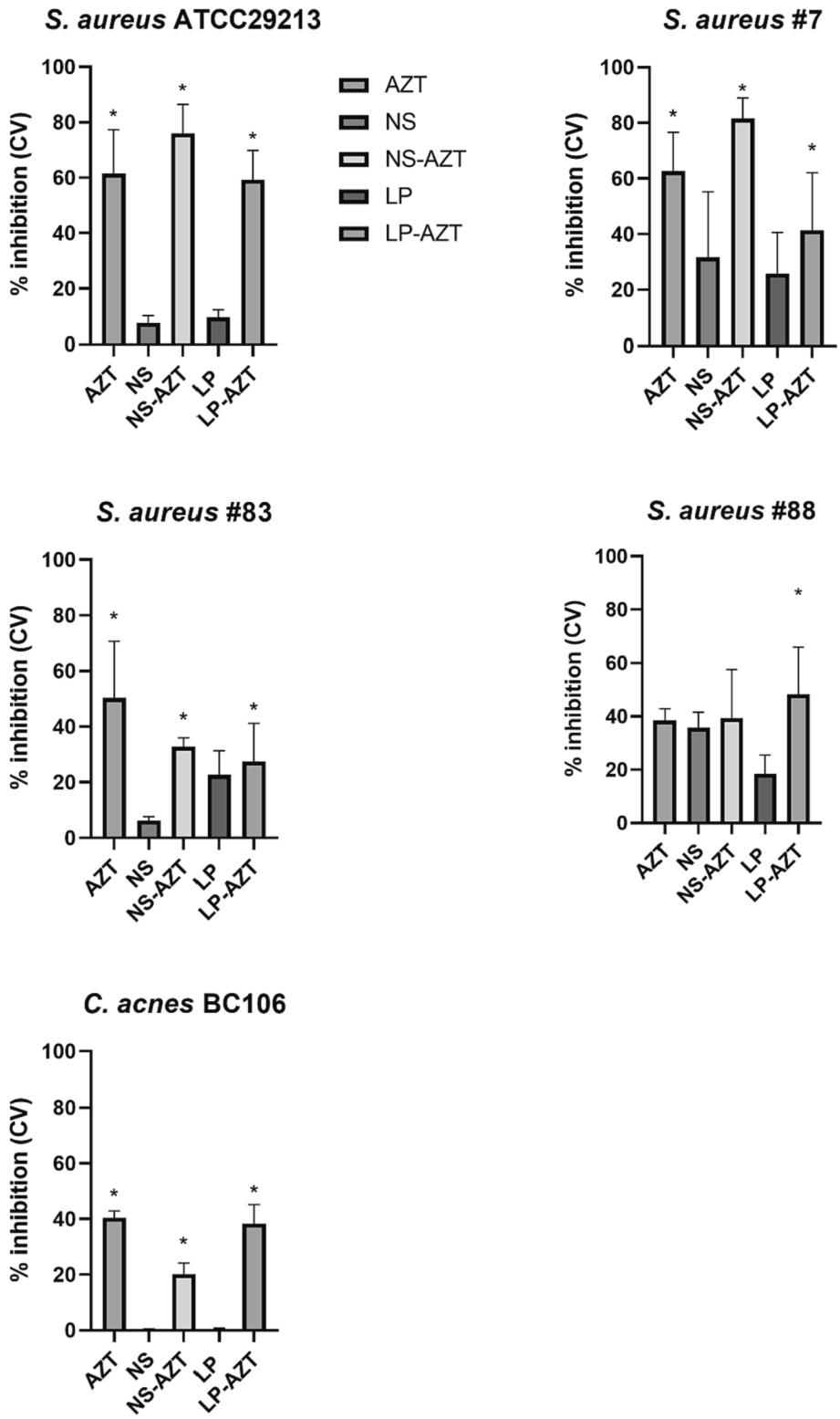

Fig. 7. Inhibition of biofilm formation exerted by AZT, unloaded LP-EPC-TFH (LP) and NS-Span 40-TFH (NS), and loaded LP-EPC-TFH (LP-AZT) and NS-Span 40-TFH (NS-AZT), administered at 2 × MIC concentrations on *S. aureus* strains and *C. acnes* BC106. Biofilms were quantified by crystal violet (CV) staining and inhibition of biofilm formation was calculated with respect to untreated biofilms. Data are expressed as means ± SD, n = 4. * $p < 0.05$ vs untreated biofilms.

the selected formulations were maintained after the storage period of 180 days at 4–8 °C, thus demonstrating that LP-EPC-TFH and NS-Span 40-TFH retained their antimicrobial activity upon storage.

To better characterize the antimicrobial properties of LP-EPC-TFH and NS-Span 40-TFH, their ability to interfere with bacterial biofilms was also investigated. Biofilm development inhibition was calculated and reported in Fig. 7. Microbial biofilms represent a major issue in topic infections and heavily impact on health care system and social costs; thus, the efficacy of a drug, also included in a delivery system, on the development of microbial biofilms is of great importance and can

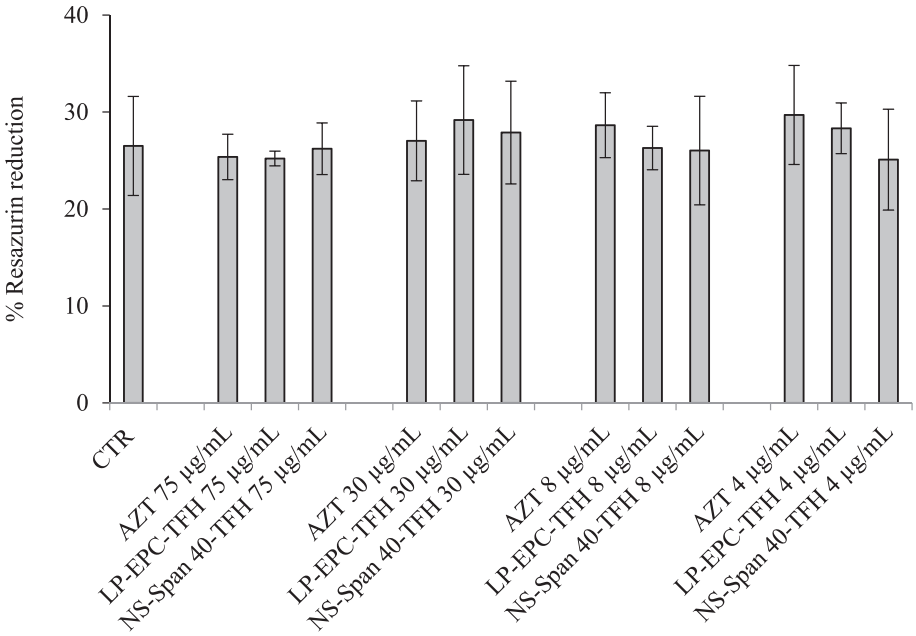

Fig. 8. The metabolic activity of human primary fibroblast cells was measured in untreated (CTR, positive metabolic control) or in treated cells with AZT solution (75, 30, 8, or 4 μg/mL), LP-EPC-TFH or NS-Span 40-TFH (containing the same concentrations of AZT) for 24 h using the Resazurin reduction-based assay. Data are expressed as mean percentages of reduced Resazurin ± standard deviations (SD), n = 3.

Table 3
Cell viability of human primary fibroblast was assessed by counting live and dead cells after 24 h of treatment with AZT solution (30 μg/mL), LP-EPC-TFH or NS-Span 40-TFH (containing the same concentrations of AZT). Untreated cells (CTR) were used as a positive viability control. Data are expressed as mean percentages of living cells /total number of cells ± standard deviations (SD), n = 3.

Group	% of living cells ÷ SD
CTR	97.05 ± 0.57
AZT 30 μg/mL	96.12 ± 1.03
LP-EPC-THF 30 μg/mL	97.81 ± 0.11
NS-Span 40-THF 30 μg/mL	97.34 ± 0.51

represent an added value. Free AZT administered at doses corresponding to 2 x MIC values, reduced biofilm formation by 50.69 % in average (range 38.43–62.74 %), depending on the microbial strain. A complete abolishment of biofilm formation was never observed at the tested concentration of drug (2 × MIC), this behaviour is not surprising since biofilm susceptibility to antibiotics is expected to be lower than planktonic cultures, mainly due to limited drug diffusion and different metabolic state of adherent cells. Unloaded LP-EPC-TFH and NS-Span 40-TFH did not significantly reduce *S. aureus* and *C. acnes* biofilm formation; AZT-loaded LP-EPC-TFH and NS-Span 40-TFH significantly inhibited bacterial biofilms and their activity is comparable to the one of free AZT for all strains ($p > 0.05$), except for LP-EPC-TFH on *S. aureus* strain #83, for which the inclusion of AZT into LP slightly decreased its effect.

3.9. Metabolic activity and cell viability in vitro assays

To evaluate the safety of AZT-loaded formulations, *in vitro* assays were performed to assess both metabolic activity and cell viability of primary fibroblasts after AZT, LP-EPC-TFH and NS-Span 40-TFH exposure. As shown in Fig. 8, when fibroblasts were incubated for 24 h with AZT solution (75, 30, 8, or 4 μg/mL), LP-EPC-TFH or NS-Span 40-TFH (containing the same concentrations of AZT), no difference was observed in cell metabolism compared to untreated cells (CTR, positive metabolic control; $p > 0.05$). These data demonstrated that the selected formulations did not alter cell functionality, thus suggesting the absence of cytotoxic effects on cells, even when the highest concentrations of AZT were used. To strengthen these results, fibroblast viability was assessed by counting live and dead cells after 24 h exposure to AZT alone, LP-EPC-TFH or NS-Span 40-TFH (30 μg/mL, selected drug concentration among all those tested since it was the first concentration higher than the MIC values measured in Section 3.8). As shown in Table 3, the percentage of living cells treated with AZT alone, LP-EPC-TFH or NS-Span 40-TFH was comparable to that of untreated cells (CTR, positive viability control) confirming the safety of the selected formulations.

4. Conclusions

Currently, bacterial skin infections are classified among the most common infections in primary care, often leading to hospital admissions. Additionally, the rapid development of multi-drug resistant bacteria has determined a higher risk of invasive disease and failure of the treatment. Among skin infections, acne vulgaris represents a common skin condition, largely affecting adolescents and young adults, which have a negative effect on their self-esteem, mood and quality of life. In this context, effective strategies are urgently sought for limiting the widespread of bacterial skin infections. In the present study, for the first time AZT based LP and NS were successfully prepared by employing two different manufacturing methods and several excipients and proposed for the treatment of skin infections and acne. Data allowed concluding that the preparation method as well as the composition influenced the functional properties of the vesicles. In general, vesicles obtained through TFH showed a larger size with respect to the vesicles obtained through EI method and determined a more sustained release of AZT. All the prepared vesicles presented a negative ζ potential, which assured their stability over the storage period. Among all the formulations, LP-EPC-TFH and NS-Span 40-TFH permitted to obtain the greatest accumulation of the drug inside the skin, determining at the same time the lowest drug absorption. They did not exhibit any cytotoxicity and retained antimicrobial activity. From all the mentioned characteristics, the selected formulations can be considered promising topical delivery

nanosystems for AZT delivery, able to improve the treatment outcomes of bacterial skin infections and acne.

CRediT authorship contribution statement

A. Abruzzo: Conceptualization, Formal analysis, Investigation, Methodology, Validation, Writing – original draft, Writing – review & editing. **R. Pucci:** Formal analysis, Investigation, Methodology, Validation. **P.M. Abruzzo:** . **S. Canaider:** Methodology, Writing – review & editing. **C. Parolin:** Conceptualization, Formal analysis, Investigation, Methodology, Validation, Writing – original draft. **B. Vitali:** Methodology, Writing – review & editing. **F. Valle:** Investigation, Writing – review & editing. **M. Brucale:** Investigation, Writing – review & editing, Formal analysis, Methodology, Validation. **T. Cerchiara:** Writing – review & editing. **B. Luppi:** Writing – review & editing. **F. Bigucci:** Conceptualization, Methodology, Writing – original draft, Writing – review & editing.

Declaration of competing interest

The authors declare that they have no known competing financial interests or personal relationships that could have appeared to influence the work reported in this paper.

Data availability

Data will be made available on request.

References

[1] L.G. Miller, D.F. Eisenberg, H. Liu, C.-L. Chang, Y. Wang, R. Luthra, A. Wallace, C. Fang, J. Singer, J.A. Suaya, Incidence of skin and soft tissue infections in ambulatory and inpatient settings, 2005–2010, BMC Infect. Dis. 15 (2015) 362, https://doi.org/10.1186/s12879-015-1071-0.

[2] V. Ki, C. Rotstein, Bacterial skin and soft tissue infections in adults: a review of their epidemiology, pathogenesis, diagnosis, treatment and site of care, Can. J. Infect. Dis. Med. Microbiol. 19 (2008) 173–184, https://doi.org/10.1155/2008/846453.

[3] P. Wolkenstein, A. Machovcová, J.C. Szepietowski, D. Tennstedt, S. Veraldi, A. Delarue, Acne prevalence and associations with lifestyle: a cross-sectional online survey of adolescents/young adults in 7 European countries, J. Eur. Acad. Dermatol. Venereol. 32 (2018) 298–306, https://doi.org/10.1111/jdv.14475.

[4] J.-P. Claudel, N. Auffret, M.-T. Leccia, F. Poli, S. Corvec, B. Dréno, *Staphylococcus epidermidis*: a potential new player in the physiopathology of acne? Dermatology 235 (2019) 287–294, https://doi.org/10.1159/000499858.

[5] N. Yamaguchi, K. Satoh-Yamaguchi, M. Ono, In vitro evaluation of antibacterial, anticollagenase, and antioxidant activities of hop components (Humulus lupulus) addressing acne vulgaris, Phytomedicine 16 (2009) 369–376, https://doi.org/10.1016/j.phymed.2008.12.021.

[6] T. Zhu, F. Fang, D. Sun, S. Yang, X. Zhang, X. Yu, L. Yang, Piceatannol inhibits P. acnes–induced keratinocyte proliferation and migration by downregulating oxidative stress and the inflammatory response, Inflammation 43 (2020) 347–357, https://doi.org/10.1007/s10753-019-01125-8.

[7] C. Folle, N. Díaz-Garrido, E. Sánchez-López, A.M. Marqués, J. Badia, L. Baldomà, M. Espina, A.C. Calpena, M.L. García, Surface-modified multifunctional thymol-loaded biodegradable nanoparticles for topical acne treatment, Pharmaceutics. 13 (2021) 1501, https://doi.org/10.3390/pharmaceutics13091501.

[8] A.S. Lee, H. de Lencastre, J. Garau, J. Kluytmans, S. Malhotra-Kumar, A. Peschel, S. Harbarth, Methicillin-resistant Staphylococcus aureus, Nat. Rev. Dis. Primer. 4 (2018) 18033, https://doi.org/10.1038/nrdp.2018.33.

[9] T.R. Walsh, J. Efthimiou, B. Dréno, Systematic review of antibiotic resistance in acne: an increasing topical and oral threat, Lancet Infect. Dis. 16 (2016) e23–e33, https://doi.org/10.1016/S1473-3099(15)00527-7.

[10] E. Elhassan, N. Devnarain, M. Mohammed, T. Govender, C.A. Omolo, Engineering hybrid nanosystems for efficient and targeted delivery against bacterial infections, J. Control. Release 351 (2022) 598–622, https://doi.org/10.1016/j.jconrel.2022.09.052.

[11] M. Sala, R. Diab, A. Elaissari, H. Fessi, Lipid nanocarriers as skin drug delivery systems: properties, mechanisms of skin interactions and medical applications, Int. J. Pharm. 535 (2018) 1–17, https://doi.org/10.1016/j.ijpharm.2017.10.046.

[12] Y.-C. Yeh, T.-H. Huang, S.-C. Yang, C.-C. Chen, J.-Y. Fang, Nano-based drug delivery or targeting to eradicate bacteria for infection mitigation: a review of recent advances, Front. Chem. 8 (2020) 286, https://doi.org/10.3389/fchem.2020.00286.

[13] J.M.V. Makabenta, A. Nabawy, C.-H. Li, S. Schmidt-Malan, R. Patel, V.M. Rotello, Nanomaterial-based therapeutics for antibiotic-resistant bacterial infections, Nat. Rev. Microbiol. 19 (2021) 23–36, https://doi.org/10.1038/s41579-020-0420-1.

[14] M. Heidary, A. Ebrahimi Samangani, A. Kargari, A. Kiani Nejad, I. Yashmi, M. Motahar, E. Taki, S. Khoshnood, Mechanism of action, resistance, synergism, and clinical implications of azithromycin, J. Clin. Lab. Anal. 36 (2022), https://doi.org/10.1002/jcla.24427.

[15] D. Bonamonte, A. De Marco, R. Giuffrida, C. Conforti, C. Barlusconi, C. Foti, P. Romita, Topical antibiotics in the dermatological clinical practice: Indications, efficacy, and adverse effects, Dermatol. Ther. 33 (2020), https://doi.org/10.1111/dth.13824.

[16] Z. Rukavina, M. Šegvić Klarić, J. Filipović-Grčić, J. Lovrić, Ž. Vanić, Azithromycin-loaded liposomes for enhanced topical treatment of methicillin-resistant Staphyloccocus aureus (MRSA) infections, Int. J. Pharm. 553 (2018) 109–119, https://doi.org/10.1016/j.ijpharm.2018.10.024.

[17] A. Abruzzo, C. Parolin, M. Rossi, B. Vitali, C. Cappadone, F. Bigucci, Development and characterization of azithromycin-loaded microemulsions: a promising tool for the treatment of bacterial skin infections, Antibiotics 11 (2022) 1040, https://doi.org/10.3390/antibiotics11081040.

[18] S. Chen, S. Hanning, J. Falconer, M. Locke, J. Wen, Recent advances in non-ionic surfactant vesicles (niosomes): fabrication, characterization, pharmaceutical and cosmetic applications, Eur. J. Pharm. Biopharm. 144 (2019) 18–39, https://doi.org/10.1016/j.ejpb.2019.08.015.

[19] D. Lombardo, M.A. Kiselev, Methods of liposomes preparation: formation and control factors of versatile nanocarriers for biomedical and nanomedicine application, Pharmaceutics. 14 (2022) 543, https://doi.org/10.3390/pharmaceutics14030543.

[20] Z. Rukavina, Ž. Vanić, Current trends in development of liposomes for targeting bacterial biofilms, Pharmaceutics. 8 (2016) 18, https://doi.org/10.3390/pharmaceutics8020018.

[21] T.T. Pham, C. Jaafar-Maalej, C. Charcosset, H. Fessi, Liposome and niosome preparation using a membrane contactor for scale-up, Colloids Surf. B Biointerfaces 94 (2012) 15–21, https://doi.org/10.1016/j.colsurfb.2011.12.036.

[22] T. Uchino, F. Lefeber, G. Gooris, J. Bouwstra, Physicochemical characterization of drug-loaded rigid and elastic vesicles, Int. J. Pharm. 412 (2011) 142–147, https://doi.org/10.1016/j.ijpharm.2011.04.016.

[23] A. Abruzzo, B. Giordani, C. Parolin, B. Vitali, M. Protti, L. Mercolini, M. Cappelletti, S. Fedi, F. Bigucci, T. Cerchiara, B. Luppi, Novel mixed vesicles containing lactobacilli biosurfactant for vaginal delivery of an anti- Candida agent, Eur. J. Pharm. Sci. 112 (2018) 95–101, https://doi.org/10.1016/j.ejps.2017.11.012.

[24] P.O. Nnamani, S. Hansen, M. Windbergs, C.-M. Lehr, Development of artemether-loaded nanostructured lipid carrier (NLC) formulation for topical application, Int. J. Pharm. 477 (2014) 208–217, https://doi.org/10.1016/j.ijpharm.2014.10.004.

[25] A. Abruzzo, C. Cappadone, G. Farruggia, B. Luppi, F. Bigucci, T. Cerchiara, Glycyrrhetinic acid liposomes and hyalurosomes on Spanish broom, flax, and hemp dressings to heal skin wounds, Molecules. 25 (2020) 2558, https://doi.org/10.3390/molecules25112558.

[26] A. Ridolfi, M. Brucale, C. Montis, L. Caselli, L. Paolini, A. Borup, A.T. Boysen, F. Loria, M.J.C. van Herwijnen, M. Kleinjan, P. Nejsum, N. Zarovni, M.H. M. Wauben, D. Berti, P. Bergese, F. Valle, AFM-based high-throughput nanomechanical screening of single extracellular vesicles, Anal. Chem. 92 (2020) 10274–10282, https://doi.org/10.1021/acs.analchem.9b05716.

[27] A. Ridolfi, L. Caselli, M. Baldoni, C. Montis, F. Mercuri, D. Berti, F. Valle, M. Brucale, Stiffness of fluid and gel phase lipid nanovesicles: weighting the contributions of membrane bending modulus and luminal pressurization, Langmuir 37 (2021) 12027–12037, https://doi.org/10.1021/acs.langmuir.1c01660.

[28] A. Ridolfi, L. Conti, M. Brucale, R. Frigerio, J. Cardellini, A. Musicò, M. Romano, A. Zendrini, L. Polito, G. Bergamaschi, A. Gori, C. Montis, S. Panella, L. Barile, D. Berti, A. Radeghieri, P. Bergese, M. Cretich, F. Valle, Particle profiling of EV-lipoprotein mixtures by AFM nanomechanical imaging, J. Extracell. Vesicles. 12 (2023) 12349, https://doi.org/10.1002/jev2.12349.

[29] D. Nečas, P. Klapetek, Gwyddion: an open-source software for SPM data analysis, Open Phys. 10 (2012), https://doi.org/10.2478/s11534-011-0096-2.

[30] A. Abruzzo, C. Cappadone, V. Sallustio, G. Picone, M. Rossi, F.P. Nicoletta, B. Luppi, F. Bigucci, T. Cerchiara, Development of spanish broom and flax dressings with glycyrrhetinic acid-loaded films for wound healing: characterization and evaluation of biological properties, Pharmaceutics. 13 (2021) 1192, https://doi.org/10.3390/pharmaceutics13081192.

[31] B. Giordani, P.E. Costantini, S. Fedi, M. Cappelletti, A. Abruzzo, C. Parolin, C. Foschi, G. Frisco, N. Calonghi, T. Cerchiara, F. Bigucci, B. Luppi, B. Vitali, Liposomes containing biosurfactants isolated from Lactobacillus gasseri exert antibiofilm activity against methicillin resistant Staphylococcus aureus strains, Eur. J. Pharm. Biopharm. 139 (2019) 246–252, https://doi.org/10.1016/j.ejpb.2019.04.011.

[32] M100 PERFORMANCE STANDARDS FOR ANTIMICROBIAL SUSCEPTIBILITY TESTING, 33RD EDITION,M100ED33, CLSI, S.l., 2023.

[33] E. Bianconi, R. Tassinari, A. Alessandrini, G. Ragazzini, C. Cavallini, P.M. Abruzzo, G. Petrocelli, L. Pampanella, R. Casadei, M. Maioli, S. Canaider, F. Facchin, C. Ventura, Cytochalasin B modulates nanomechanical patterning and fate in human adipose-derived stem cells, Cells. 11 (2022) 1629, https://doi.org/10.3390/cells11101629.

[34] L. Pampanella, P.M. Abruzzo, R. Tassinari, A. Alessandrini, G. Petrocelli, G. Ragazzini, C. Cavallini, V. Pizzuti, N. Collura, S. Canaider, F. Facchin, C. Ventura, Cytochalasin B influences cytoskeletal organization and osteogenic potential of human Wharton's jelly mesenchymal stem cells, Pharmaceuticals. 16 (2023) 289, https://doi.org/10.3390/ph16020289.

[35] P. Liu, G. Chen, J. Zhang, A review of liposomes as a drug delivery system: current status of approved products, regulatory environments, and future perspectives, Molecules. 27 (2022) 1372, https://doi.org/10.3390/molecules27041372.
[36] A. Gouda, O.S. Sakr, M. Nasr, O. Sammour, Ethanol injection technique for liposomes formulation: an insight into development, influencing factors, challenges and applications, J. Drug Deliv. Sci. Technol. 61 (2021) 102174, https://doi.org/10.1016/j.jddst.2020.102174.
[37] A. Abruzzo, B. Giordani, C. Parolin, P.R. De Gregorio, C. Foschi, T. Cerchiara, F. Bigucci, B. Vitali, B. Luppi, Lactobacillus crispatus BC1 biosurfactant delivered by hyalurosomes: an advanced strategy to counteract candida biofilm, Antibiotics 10 (2021) 33, https://doi.org/10.3390/antibiotics10010033.
[38] D. Verma, Particle size of liposomes influences dermal delivery of substances into skin, Int. J. Pharm. 258 (2003) 141–151, https://doi.org/10.1016/S0378-5173(03)00183-2.
[39] S. Sahudin, N. Sahrum Ayumi, N. Kaharudin, Enhancement of skin permeation and penetration of β-arbutin fabricated in chitosan nanoparticles as the delivery system, Cosmetics 9 (2022) 114, https://doi.org/10.3390/cosmetics9060114.
[40] M. Danaei, M. Dehghankhold, S. Ataei, F. Hasanzadeh Davarani, R. Javanmard, A. Dokhani, S. Khorasani, M. Mozafari, Impact of particle size and polydispersity index on the clinical applications of lipidic nanocarrier systems, Pharmaceutics. 10 (2018) 57, https://doi.org/10.3390/pharmaceutics10020057.
[41] M. Al-Amin, F. Bellato, F. Mastrotto, M. Garofalo, A. Malfanti, S. Salmaso, P. Caliceti, Dexamethasone loaded liposomes by thin-film hydration and microfluidic procedures: formulation challenges, Int. J. Mol. Sci. 21 (2020) 1611, https://doi.org/10.3390/ijms21051611.
[42] T.T. Duong, A. Isomäki, U. Paaver, I. Laidmäe, A. Tõnisoo, T.T.H. Yen, K. Kogermann, A. Raal, J. Heinämäki, T.-M.-H. Pham, Nanoformulation and evaluation of oral berberine-loaded liposomes, Molecules 26 (2021) 2591, https://doi.org/10.3390/molecules26092591.
[43] M. Manconi, C. Sinico, D. Valenti, G. Loy, A.M. Fadda, Niosomes as carriers for tretinoin. I. Preparation and properties, Int. J. Pharm. 234 (2002) 237–248, https://doi.org/10.1016/S0378-5173(01)00971-1.
[44] M. Nasr, S. Mansour, N.D. Mortada, A.A. Elshamy, Vesicular aceclofenac systems: a comparative study between liposomes and niosomes, J. Microencapsul. 25 (2008) 499–512, https://doi.org/10.1080/02652040802055411.
[45] S. Melchior, M. Codrich, A. Gorassini, D. Mehn, J. Ponti, G. Verardo, G. Tell, L. Calzolai, S. Calligaris, Design and advanced characterization of quercetin-loaded nano-liposomes prepared by high-pressure homogenization, Food Chem. 428 (2023) 136680, https://doi.org/10.1016/j.foodchem.2023.136680.
[46] M.L. Manca, E. Casula, F. Marongiu, G. Bacchetta, G. Sarais, M. Zaru, E. Escribano-Ferrer, J.E. Peris, I. Usach, S. Fais, A. Scano, G. Orrù, R.G. Maroun, A.M. Fadda, M. Manconi, From waste to health: sustainable exploitation of grape pomace seed extract to manufacture antioxidant, regenerative and prebiotic nanovesicles within circular economy, Sci. Rep. 10 (2020) 14184, https://doi.org/10.1038/s41598-020-71191-8.
[47] A. Gillet, P. Compère, F. Lecomte, P. Hubert, E. Ducat, B. Evrard, G. Piel, Liposome surface charge influence on skin penetration behaviour, Int. J. Pharm. 411 (2011) 223–231, https://doi.org/10.1016/j.ijpharm.2011.03.049.
[48] Z. Németh, I. Csóka, R. Semnani Jazani, B. Sipos, H. Haspel, G. Kozma, Z. Kónya, D. G. Dobó, Quality by design-driven zeta potential optimisation study of liposomes with charge imparting membrane additives, Pharmaceutics. 14 (2022) 1798, https://doi.org/10.3390/pharmaceutics14091798.
[49] H.M. Hnin, E. Stefánsson, T. Loftsson, R. Asasutjarit, D. Charnvanich, P. Jansook, Physicochemical and stability evaluation of topical niosomal encapsulating fosinopril/γ-cyclodextrin complex for ocular delivery, Pharmaceutics. 14 (2022) 1147, https://doi.org/10.3390/pharmaceutics14061147.
[50] E. Judy, M. Lopus, N. Kishore, Mechanistic insights into encapsulation and release of drugs in colloidal niosomal systems: biophysical aspects, RSC Adv. 11 (2021) 35110–35126, https://doi.org/10.1039/D1RA06057K.
[51] P. Balakrishnan, S. Shanmugam, W.S. Lee, W.M. Lee, J.O. Kim, D.H. Oh, D.-D. Kim, J.S. Kim, B.K. Yoo, H.-G. Choi, J.S. Woo, C.S. Yong, Formulation and in vitro assessment of minoxidil niosomes for enhanced skin delivery, Int. J. Pharm. 377 (2009) 1–8, https://doi.org/10.1016/j.ijpharm.2009.04.020.
[52] M.S. Saddik, M.M.A. Elsayed, M.A. El-Mokhtar, H. Sedky, J.A. Abdel-Aleem, A. M. Abu-Dief, M.F. Al-Hakkani, H.L. Hussein, S.A. Al-Shelkamy, F.Y. Meligy, A. Khames, H.A. Abou-Taleb, Tailoring of novel azithromycin-loaded zinc oxide nanoparticles for wound healing, Pharmaceutics. 14 (2022) 111, https://doi.org/10.3390/pharmaceutics14010111.
[53] I.A. Alvi, J. Madan, D. Kaushik, S. Sardana, R.S. Pandey, A. Ali, Comparative study of transfersomes, liposomes, and niosomes for topical delivery of 5-fluorouracil to skin cancer cells: preparation, characterization, in-vitro release, and cytotoxicity analysis, Anticancer Drugs 22 (2011) 774–782, https://doi.org/10.1097/CAD.0b013e328346c7d6.
[54] D.V. Bhalani, B. Nutan, A. Kumar, A.K. Singh Chandel, Bioavailability enhancement techniques for poorly aqueous soluble drugs and therapeutics, Biomedicines 10 (2022) 2055, https://doi.org/10.3390/biomedicines10092055.
[55] D. Vorselen, M. Marchetti, C. López-Iglesias, P.J. Peters, W.H. Roos, G.J.L. Wuite, Multilamellar nanovesicles show distinct mechanical properties depending on their degree of lamellarity, Nanoscale 10 (2018) 5318–5324, https://doi.org/10.1039/C7NR09224E.
[56] G. Shilakari Asthana, P.K. Sharma, A. Asthana, *In Vitro* and *In Vivo* evaluation of niosomal formulation for controlled delivery of clarithromycin, Scientifica 2016 (2016) 1–10. 10.1155/2016/6492953.
[57] N. Raina, R. Rani, V.K. Thakur, M. Gupta, New insights in topical drug delivery for skin disorders: from a nanotechnological perspective, ACS Omega 8 (2023) 19145–19167, https://doi.org/10.1021/acsomega.2c08016.
[58] L.M. Ickenstein, M.C. Sandström, L.D. Mayer, K. Edwards, Effects of phospholipid hydrolysis on the aggregate structure in DPPC/DSPE-PEG2000 liposome preparations after gel to liquid crystalline phase transition, Biochim. Biophys. Acta BBA - Biomembr. 1758 (2006) 171–180, https://doi.org/10.1016/j.bbamem.2006.02.016.
[59] P. Nakhaei, R. Margiana, D.O. Bokov, W.K. Abdelbasset, M.A. Jadidi Kouhbanani, R.S. Varma, F. Marofi, M. Jarahian, N. Beheshtkhoo, Liposomes: structure, biomedical applications, and stability parameters with emphasis on cholesterol, Front. Bioeng. Biotechnol. 9 (2021) 705886, https://doi.org/10.3389/fbioe.2021.705886.
[60] A. Memoli, L.G. Palermiti, V. Travagli, F. Alhaique, Lipid peroxidation of L-α-phosphatidylcholine from fresh egg yolk and from soybean during liposome preparation and storage, J. Liposome Res. 3 (1993) 697–706, https://doi.org/10.3109/08982109309150752.
[61] M. Gupta, B. Vaidya, N. Mishra, S.P. Vyas, Effect of surfactants on the characteristics of fluconazole niosomes for enhanced cutaneous delivery, Artif. Cells Blood Substit. Biotechnol. 39 (2011) 376–384, https://doi.org/10.3109/10731199.2011.611476.
[62] M.F. Peralta, M.L. Guzmán, A.P. Pérez, G.A. Apezteguia, M.L. Fórmica, E. L. Romero, M.E. Olivera, D.C. Carrer, Liposomes can both enhance or reduce drugs penetration through the skin, Sci. Rep. 8 (2018) 13253, https://doi.org/10.1038/s41598-018-31693-y.
[63] The European Committee on Antimicrobial Susceptibility Testing. Routine and extended internal quality control for MIC determination and disk diffusion as recommended by EUCAST, (n.d.).
[64] A.B. Scriboni, V.M. Couto, L.N. De Morais Ribeiro, I.A. Freires, F.C. Groppo, E. De Paula, M. Franz-Montan, K. Cogo-Müller, Fusogenic liposomes increase the antimicrobial activity of vancomycin against staphylococcus aureus biofilm, Front. Pharmacol. 29 (10) (2019) 1401.